

New Interaction Parameters for Oxygen Compounds in the GROMOS Force Field: Improved Pure-Liquid and Solvation Properties for Alcohols, Ethers, Aldehydes, Ketones, Carboxylic Acids, and Esters

Bruno A. C. Horta,^{†,*} Patrick F. J. Fuchs,^{‡,§,||} Wilfred F. van Gunsteren,[†] and Philippe H. Hünenberger^{†,*}

[†]Laboratory of Physical Chemistry, ETH Zürich, CH-8093 Zürich, Switzerland

[‡]INSERM UMR-S665, DSIMB, Paris, France

[§]Université Paris-Diderot, UFR Sciences du Vivant, Paris, France

^{||}Institut National de Transfusion Sanguine, Paris, France

ABSTRACT: A new parameter set (S3A6_{OXY}) is developed for the GROMOS force field, that combines reoptimized parameters for the oxygen-containing chemical functions (alcohols, ethers, aldehydes, ketones, carboxylic acids, and esters) with the current biomolecular force field version (S3A6) for all other functions. In the context of oxygen-containing functions, the S3A6_{OXY} parameter set is obtained by optimization of simulated pure-liquid properties, namely the density ρ_{liq} and enthalpy of vaporization ΔH_{vap} , as well as solvation properties, namely the free energies of solvation in water ΔG_{wat} and in cyclohexane ΔG_{che} , against experimental data for 10 selected organic compounds, and further tested for 25 other compounds. The simultaneous refinement of atomic charges and Lennard-Jones interaction parameters against the four mentioned types of properties provides a single parameter set for the simulation of both liquid and biomolecular systems. Small changes in the covalent parameters controlling the geometry of the oxygen-containing chemical functions are also undertaken. The new S3A6_{OXY} force-field parameters reproduce the mentioned experimental data within root-mean-square deviations of 22.4 kg m^{-3} (ρ_{liq}), 3.1 kJ mol^{-1} (ΔH_{vap}), 3.0 kJ mol^{-1} (ΔG_{wat}), and 1.7 kJ mol^{-1} (ΔG_{che}) for the 35 compounds considered.

I. INTRODUCTION

Molecular dynamics (MD) simulation represents a powerful tool for investigating the properties of molecular systems relevant in physics, chemistry, and biology.^{1–4} The usefulness of this method in the context of condensed-phase systems results in particular from a favorable trade-off between model resolution and computational cost. Although classical atomistic models represent an approximation to quantum mechanics (QM), they can still provide a realistic description of molecular systems at spatial and temporal resolutions on the order of 0.1 nm and 1 fs, respectively, while their computational cost remains tractable at present for system sizes and time scales on the order of 10 nm and 100 ns, respectively. These scales are sufficient to enable in many cases (i) an appropriate description of solvation, by explicit treatment of the solvent molecules within a sufficiently large solvation range; (ii) a reliable calculation of thermodynamic properties *via* statistical mechanics; and (iii) a direct comparison with experimental data, namely structural, thermodynamic, transport, and dynamic observables measured on similar spatial and temporal scales.

In classical MD simulations, the atomic coordinates and velocities are propagated in time by integrating Newton's equations of motion, possibly thermostatted and barostatted,⁵ and reformulated in a discretized form.^{6–8} To this purpose, the forces acting on each atom at a given time step are calculated on the basis of an empirical potential-energy function, also called a force field. A force field is a parametric function of the coordinates of all atoms, and its specification requires the choice of a functional form and of the associated parameter set. The

functional form is typically defined by a sum of bonded and nonbonded terms designed to model certain types of physical interactions. The bonded terms are intramolecular and generally depend each on a single internal coordinate defined by a limited set of covalently bonded atoms, e.g., bond stretching, bond-angle bending, improper-dihedral-angle distortion, and dihedral-angle torsion. The nonbonded terms account for through-space interactions and generally depend each on a single interatomic distance, e.g., pairwise electrostatic and van der Waals interactions. The parameter set consists of a list of constants involved in the evaluation of the different force-field terms, e.g., reference internal-coordinate values, force constants, torsional-potential multiplicities and phase shifts, atomic charges, and pairwise van der Waals interaction parameters.

From a broad perspective, one may distinguish between two main classes of force fields, involving different scopes and design strategies. On one hand, molecular mechanics or spectroscopic force fields, e.g., CFF,^{9,10} CVFF,¹¹ MM3,^{12–14} and MM4,¹⁵ mainly aim at an accurate description of molecular properties in the gas phase, e.g., geometries, energies, and vibrational properties. They usually involve few atom types, a complex functional form, e.g., including anharmonicities and couplings in the bonded terms, largely automated parametrization procedures, and parameters mainly derived on the basis of spectroscopic measurements and QM calculations in the gas phase. These force fields typically focus on intramolecular

Received: November 8, 2010

Published: March 25, 2011

	bond type	bond-angle type	improper-dihedral-angle type	dihedral-angle type
alcohols				
ethers				
aldehydes				
ketones				
carboxylic acids				
esters				

Figure 1. Bonded interaction types (bond stretching, bond-angle bending, improper-dihedral-angle distortion, and dihedral-angle torsion) used in the S3A6_{OXY} parameter set. The numbering refers to the type codes of the S3A5 and S3A6 parameter sets.³⁴ The corresponding parameters are also listed in Table 3.

rather than on intermolecular interactions. Due to the often simplistic representation of long-range nonbonded interactions and solvation effects, their application is usually restricted to the conformational analysis of small molecules, as a classical alternative to more expensive QM calculations. On the other hand, condensed-phase or biomolecular force fields, e.g., CHARMM,^{16–19} AMBER,^{20–23} OPLS,^{24–27} and GROMOS,^{7,28–38} mainly aim at the description of (bio)molecules in solution. They usually involve a larger number of atom types, accounting for atoms in different chemical environments, a simpler functional form, empirical parametrization procedures, a more extensive use of parameter-combination and transferability assumptions, and, in particular for OPLS and GROMOS, parameters derived mainly from experimental spectroscopic and thermodynamic data concerning liquids and solutions. These force fields focus on the description of torsional-angle properties, nonbonded interactions, and solvation effects. For this reason, they are able to capture the main physics underlying the properties of condensed-phase systems such as solids, liquids, solutions, and solvated (bio)molecules.

The GROMOS force field belongs to the second category. It has been widely used in simulations of liquids,^{39,40} crystals,^{41,42} and solutions,^{43,44} and in the context of biomolecular systems, e.g., peptides^{45,46} and proteins,^{47,48} nucleic acids,^{35,49} carbohydrates,^{50,51} and lipids.^{52,53}

The main principles underlying the construction of this force field can be summarized as follows: (i) united atom representation of aliphatic CH, CH₂, CH₃, and CH₄ groups;^{28,30,31} (ii) quartic bond-stretching (since 1996), cosine-harmonic bond-angle bending (since 1996), cosine-series dihedral-angle torsion, and harmonic improper-dihedral-angle distortion terms; (iii) Lennard-Jones representation of the van der Waals interactions; (iv) mean-field representation of electronic polarization effects *via* enhanced atomic charges appropriate for condensed-phase (polar) environments (see also refs 54–57 for recent developments concerning explicit polarization); (v) nonbonded exclusion of first and second covalent neighbors; (vi) van der Waals interaction reduction for third covalent neighbors using a special set of parameters; (vii) van der Waals interaction adjustment distinguishing between non-hydrogen-bonding, uncharged hydrogen-bonding, and charged hydrogen-bonding interactions; (viii) application of a geometric-mean combination rule⁷ for van der Waals interaction parameters of particular sets of atoms; and (ix) freely adjustable atomic partial charges; i.e., these charges are not determined by the atom type.

The main principles underlying the parametrization strategy of the force field can be summarized as follows: (i) steady but controlled parameter refinement over the years based on small molecule data and avoiding unnecessary complexity increases;

Table 1. Summary of the Main GROMOS Force-Field Versions since the Original 37C4 Parameter Set

GROMOS force field nomenclature	year of release	main improvements	references
37C4	1987	GROMOS87 force field	ref 60
43A1	1996	GROMOS96 force field	refs 7, 28
43A2	2000	reparametrization of the dihedral-angle potentials for <i>n</i> -alkanes	ref 30
45A3	2001	improved description of liquid aliphatic hydrocarbons and alkane–water systems	ref 31
45A4	2005	improved description of lipids, nucleic acids, and carbohydrates together with slight readjustment in the choice of vdW interaction types	refs 32, 35, 36, 87
53A5	2004	reoptimization of the polar functional groups (vdW and charges) for pure liquids	ref 34
53A6	2004	reoptimization of the polar functional groups (charges only; vdW identical to 53A5) based on hydration free energies	ref 34
53A6 _{OL3/Chiu}	2009	improved parameters for phosphatidylcholine bilayers	ref 38
53A6 _{OXY}	2011	reoptimization of nonbonded interaction parameters for oxygen compounds (+ slight readjustments of reference bond lengths and angles within oxygen functions)	present work

(ii) principal focus on torsional-angle properties, nonbonded interactions, and solvation effects, most relevant for the description of condensed-phase and biomolecular systems; (iii) calibration involving in the first place primary experimental data, i.e., observed thermodynamic and spectroscopic properties concerning small molecules in the condensed phase; (iv) an assumption of transferability, justifying the application of parameters calibrated for small molecules to corresponding fragments within larger molecules; (v) compatibility with the simple-point-charge (SPC) water model;⁵⁸ and (vi) compatibility with reaction-field electrostatics⁵⁹ based on an effective long-range cutoff distance of 1.4 nm (since 1996).

The original 37C4 version of the GROMOS force field⁶⁰ (see refs 7, 34, 61 for a historical overview) has been progressively refined and extended, still maintaining the compatibility with the original functional form, except for the change^{7,8,29} to quartic bond stretching, cosine-harmonic bond-angle bending, and reaction field electrostatics in 1996, and the SPC water model.⁵⁸ The main consecutive versions of the force field are listed in Table 1. These were validated by simulations of liquids and solvated biomolecules.^{44,62,63} A complete description of the functional form of the GROMOS force field can be found in refs 7, 8, 29, and 34. The most recent published force-field parameter sets are labeled 53A5 and 53A6 and have been described by Oostenbrink et al.³⁴

The latest force-field version includes two distinct parameter sets, exclusively differing in the atomic partial charges within polar functional groups. Set 53A5, which was parametrized to reproduce thermodynamic properties, e.g., densities and enthalpies of vaporization, of pure liquids, is recommended for the simulation of organic liquids and liquid mixtures. Set 53A6, in which the atomic partial charges were readjusted so as to reproduce hydration free energies of polar amino acid analogs, is recommended for the simulations of biomolecular systems. The decision of providing two distinct parameter sets³⁴ resulted from the apparent impossibility of reproducing pure-liquid properties and hydration free energies simultaneously with a sufficient accuracy. This incompatibility may be an unavoidable consequence of the mean-field treatment of electronic polarization, rendering the derivation of parameters appropriate for both highly polar (aqueous solution) and less polar (pure organic liquids) environments impossible. However, two considerations may soften this statement. First, the derivation of set 53A6 only involved a readjustment of the charges, not of the van der Waals interaction parameters. Thus, this set may be viewed as a compromise combining charges appropriate for high-polarity

environments with van der Waals interaction parameters appropriate for lower-polarity environments. For this reason, it has been recommended, rather than set 53A5, for the simulation of systems where the partitioning of polar functional groups between polar and nonpolar environments is of relevance, e.g., biomolecules. This compromise is, however suboptimal, compared to allowing for the flexibility that would be offered by a simultaneous refinement of the two types of nonbonded interaction parameters. Second, the derivation of the common van der Waals interaction parameters of the two sets only involved the adjustment of the repulsive (C_{12}) coefficients of the Lennard-Jones interaction, not of the corresponding dispersive (C_6) coefficients. The reason for the latter choice was the qualitative connection existing between pairwise dispersive interactions and the electronic polarizabilities of the involved atoms, e.g., through the Slater–Kirkwood expression,⁶⁴ which suggests that the C_6 parameters should not be freely adjustable. However, considering that the original GROMOS C_6 parameters⁷ have been derived on the basis of gas-phase atomic polarizabilities, which might differ from the “effective” polarizabilities of atoms in molecular environments, limited adjustments of these parameters might be physically justified and used to further enhance the agreement with the target data.

The goal of the present work is to consistently reoptimize the nonbonded interaction parameters of set 53A6, in order to derive a new parameter set reconciling the reproduction of experimental data concerning pure organic liquids as well as aqueous and nonaqueous solvation properties within a reasonable accuracy, namely, as measured by root-mean-square deviations, on the order of a few percent (about 1–3%) in terms of densities and of $k_B T$ (2.5 kJ mol^{−1} at room temperature) in terms of energetic properties. This is done by allowing more force-field parameters to be optimized than was the case in the calibration of the 53A5 and 53A6 versions of the force field. At present, solely oxygen compounds are considered, including the most common chemical functions of the elements C, H, and O, namely, alcohols, ethers, aldehydes, ketones, carboxylic acids, and esters. The refinement only affects the atomic partial charges within the above functions and the parameters for van der Waals interactions involving oxygen atoms. A slight readjustment in the reference values (but not force constants) of the bond-stretching and bond-angle-bending terms within these functions is also undertaken, so as to improve the description of their geometries. The resulting parameter set is referred to as 53A6_{OXY}.

Table 2. List of Oxygen Compounds Considered in This Study^a

chemical function	code	name	calibration ^b	ϵ_{rf}	$\kappa_{\text{T}} [10^{-4} (\text{kJ mol}^{-1} \text{nm}^{-3})^{-1}]$
alcohols	MTL	methanol		33.5	12.48
	ETL	ethanol	×	24.0	11.53
	PPL	propanol	×	20.0	10.26
	BTL	butanol		17.7	9.42
	PTL	pentanol		15.1	8.84
	HXL	hexanol		13.0	8.24
	HPL	heptanol		11.5	7.94 ^c
	OTL	octanol		10.1	7.64
	2PPL	propan-2-ol		19.1	13.32
	2BTL	butan-2-ol		16.7	9.42 ^c
	2PTL	pentan-2-ol		13.8	8.84 ^c
	3PTL	pentan-3-ol		13.4	8.84 ^c
	CHXL	cyclohexanol		16.4	8.24 ^c
	2M2P	2-methylpropan-2-ol		11.5	9.42 ^c
	2M2B	2-methylbutan-2-ol		5.7	8.84 ^c
ethers	DME	methoxymethane	×	6.2	8.00 ^c
	DEE	ethoxyethane	×	4.2	8.00 ^c
	MPH	1-methoxypropane		4.2 ^c	8.00 ^c
	DXE	1,2-dimethoxyethane		7.3	8.00 ^c
aldehydes	EAL	acetaldehyde	×	21.1	8.00 ^c
	PAL	propionaldehyde		18.4	8.00 ^c
	BAL	butyraldehyde		13.4	8.00 ^c
ketones	PPN	propanone	×	20.8	13.24
	BTN	butanone	×	17.7	11.88
	2PN	pentan-2-one		15.4	10.92
	3PN	pentan-3-one		16.6	10.92 ^c
	2HN	hexan-2-one		14.5	10.12
	3HN	hexan-3-one		14.5 ^c	10.12 ^c
acids	ACA	acetic acid	×	6.2	9.17
	PPA	propionic acid		3.4	9.29
	BTA	butyric acid		2.9	9.29 ^c
esters	EAE	ethylacetate	×	6.0	8.98 ^d
	PAE	propylacetate	×	5.6	8.67 ^d
	BAE	butylacetate		5.1	8.39 ^d
	MPE	methylpropionate		6.0	8.98 ^c

^a The acronyms adopted in this article and the official IUPAC names are provided. The values of the reaction-field static relative dielectric permittivity (ϵ_{rf}) used in the simulations are also listed and were taken from experimental results,⁸⁸ when available. The values of the isothermal compressibility κ_{T} used for the pressure scaling in the simulations are also provided and were taken from experimental results,⁶⁵ when available. ^b Compounds used in the calibration. ^c Not available experimentally and chosen on the basis of experimental data for similar compounds. ^d Not available experimentally and approximated by the corresponding adiabatic compressibility.

II. COMPUTATIONAL DETAILS

II.1. Parametrization Strategy. The 35 oxygen compounds considered in the present study are listed in Table 2, along with corresponding acronyms used in the article. With the exception of DME (boiling point⁶⁵ $T_{\text{b}} = 254$ K), all are in the liquid phase under standard conditions, i.e. at 1 bar and 298.15 K. Some of these compounds, indicated by the symbol “×”, were used in the parameter calibration, while others were only used to test the transferability of the reoptimized parameters. For example, ETL and PPL were selected to calibrate the alcohol parameters, while the 13 remaining alcohols were used for validation only.

The thermodynamic observables against which the parametrization was performed are (i) the density ρ_{liq} of the pure liquid, (ii) the enthalpy of vaporization ΔH_{vap} of the pure liquid, (iii) the solvation free energy ΔG_{wat} of the compound in water, and (iv) the solvation free energy ΔG_{che} of the compound in cyclohexane. The comparison between simulated and experimental values was performed under standard conditions, except for DME, where a temperature of 254 K was selected instead.

The improper-dihedral-angle distortion parameters, the dihedral-angle-torsion parameters, the definition of charge groups, and the special third-neighbor van der Waals interaction parameters were kept unaltered with respect to the S3A6 force field.³⁴

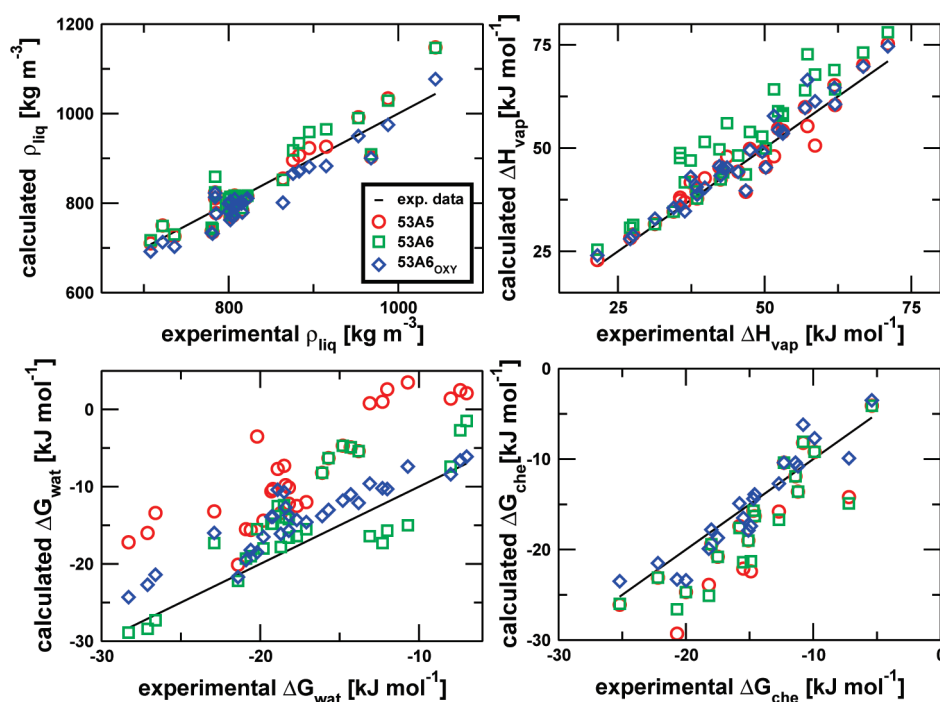


Figure 2. Comparison of simulated and experimental properties obtained with different GROMOS parameter sets (53A5, 53A6, and 53A6_{OXY}). The properties considered are the pure-liquid density ρ_{liq} and enthalpy of vaporization ΔH_{vap} as well as the solvation free energies in water ΔG_{wat} and in cyclohexane ΔG_{che} at 1 bar and 298.15 K. The straight line corresponds to a perfect agreement with experimental data.

On the other hand, the bond-stretching and bond-angle bending parameters were reassigned (from the list of existing covalent parameters), on the basis of the consideration of quantum-mechanically optimized molecular geometries (MP2/6-311++G**), as detailed in Figure 1 and Table 3. These calculations were performed using the Gaussian 03 program,⁶⁶ and the adjustment was performed on the basis of the optimized geometries of the compounds propanol, ethoxyethane, propionaldehyde, butanone, propionic acid, and ethylacetate.

The interaction parameters of the united aliphatic-carbon atoms (CH, CH₂, and CH₃) were not altered in the present work. These parameters have been previously optimized in the context of linear, branched, and cyclic alkanes against experimental pure-liquid properties, e.g., density and vaporization enthalpy, as well as hydration free energies.^{30,31} They were subsequently shown to reproduce very well other experimental properties, including solvation free energies in apolar^{44,67} and other polar solvents,⁴⁴ and conformational properties of hydrocarbons.³⁰ These parameters have been validated in the context of biomolecular simulations, and especially of lipids, e.g., in terms of melting temperatures for monoglycerides at different hydration levels.⁶⁸ Therefore, the quality of the united-aliphatic-atom parameters was not questioned, and these parameters were directly used as a starting point for the present reoptimization concerning oxygen-containing compounds.

In GROMOS, the van der Waals interactions are calculated according to a Lennard-Jones function, i.e., as

$$V^{\text{LJ}}(\mathbf{r}; C_{12}, C_6) = \sum_i \sum_{j>i} \left(\frac{C_{12,ij}}{r_{ij}^{12}} - \frac{C_{6,ij}}{r_{ij}^6} \right) \quad (1)$$

where r_{ij} is the (minimum-image) distance between two interaction sites i and j , and the parameters $C_{12,ij}$ and $C_{6,ij}$ are defined

following a geometric-mean combination rule

$$C_{12,ij} = C_{12,ii}^{1/2} C_{12,jj}^{1/2} \text{ and } C_{6,ij} = C_{6,ii}^{1/2} C_{6,jj}^{1/2} \quad (2)$$

Up to three different $C_{12}^{1/2}$ parameters are actually defined for every type of atom, labeled here $C_{12,\text{I}}^{1/2}$, $C_{12,\text{II}}^{1/2}$, and $C_{12,\text{III}}^{1/2}$. The $C_{12,\text{I}}^{1/2}$, $C_{12,\text{II}}^{1/2}$, and $C_{12,\text{III}}^{1/2}$, normally corresponding to increasing repulsiveness, are used in the cases of non-hydrogen bonding, uncharged hydrogen-bonding, or charged hydrogen-bonding interactions, respectively. In the present work, all compounds considered are uncharged, and the $C_{12,\text{III}}^{1/2}$ is not relevant. The choice of the appropriate type of $C_{12}^{1/2}$ parameter for the interaction between two given types of atoms is defined by a combination matrix (refer to Table 8 of ref 34 for the 53A5/53A6 combination matrix, which is used in the present work).

The calibration procedure involved the refinement of the Lennard-Jones interaction parameters $C_6^{1/2}$, $C_{12,\text{I}}^{1/2}$, and $C_{12,\text{II}}^{1/2}$ associated with the atom types O (carbonyl oxygen), OA (alcohol or carboxylic acid oxygen), and OE (ether or ester oxygen), as well as of the partial charges of all of the atoms involved in a specific functional group. Distinct charge sets for alcohol, ether, aldehyde, ketone, carboxylic acid, and ester groups were used. The adjustment of the $C_6^{1/2}$ parameters was kept minimal, considering the qualitative connection that exists between this parameter and the electronic polarizability of the corresponding atom.⁶⁴

The calibration was performed by trial and error, steered to some extent by chemical intuition, and a roughly incremental approach. In particular, the Lennard-Jones interaction parameters refined for oxygen atoms in alcohols (OA), ethers (OE), and ketones (O) were used directly for aldehydes, carboxylic acids, and esters. The charge sets were refined separately for the six classes of compounds. During the parametrization of some of the alcohols and carboxylic acids, adequate parameters leading to

Table 3. Bonded Interaction Parameters (Bond Stretching, Bond-Angle Bending, Improper-Dihedral-Angle Distortion, and Dihedral-Angle Torsion) Used in the S3A6_{OXY} Parameter Set and Comparison with the Values Obtained from *ab Initio* Quantum-Mechanical Geometry Optimization

bond type code	K_b [10^6 kJ mol ⁻¹ nm ⁻⁴]	bond stretching		
		b_0 [nm]	b_{eq} (HF/6-31+G**) [nm]	b_{eq} (MP2/6-311++G**) [nm]
1	15.7	0.100	0.094 ^a /0.095 ^b	0.096 ^a /0.097 ^b
3	12.3	0.109	0.110 ^c	0.111 ^c
5	16.6	0.123	0.119 ^c /0.119 ^d /0.119 ^b /0.119 ^e	0.121 ^c /0.122 ^d /0.121 ^b /0.122 ^e
13	10.2	0.136	0.133 ^b /0.132 ^c	0.136 ^b /0.136 ^c
18	8.18	0.143	0.141 ^a /0.140 ^f /0.143 ^e	0.143 ^a /0.142 ^f /0.145 ^e
27	7.15	0.153	0.151–0.153 ^{a,b,c,d,e,f}	0.151–0.153 ^{a,b,c,d,e,f}

angle type code	K_θ [kJ mol ⁻¹]	bond-angle bending		
		θ_0 [deg]	θ_{eq} (HF/6-31+G**) [degree]	θ_{eq} (MP2/6-311++G**) [degree]
12	450	109.5	110.6 ^a /108.9 ^b	107.5 ^a /105.8 ^b
15	530	111.0	108.4–114.0 ^{a,b,c,d,e,f}	108.1–113.1 ^{a,b,c,d,e,f}
16	545	113.0	111.9 ^b /112.8 ^c	111.2 ^b /111.8 ^c
21	620	116.0	116.5 ^c /115.8 ^d	115.9 ^c /116.0 ^d
22	635	117.0	117.8 ^c	114.9 ^c
25	505	120.0	119.9 ^c	120.2 ^c
31	700	122.0	122.1 ^d /122.1 ^b /123.4 ^e	122.0 ^d /122.7 ^b /123.5 ^e
33	730	124.0	123.6 ^c	123.9 ^c
35	750	125.0	126.1 ^b /123.8 ^c	126.1 ^b /124.7 ^c

improper dihedral-angle type code	improper dihedral-angle distortion	
	K_ξ [kJ mol ⁻¹ deg ⁻²]	ξ_0 [deg]
1	0.0510	0.0

dihedral-angle torsion type code	dihedral-angle torsion		
	K_ϕ [kJ mol ⁻¹]	$\cos(\delta)$	m
12	16.7	–1.0	2
23	1.26	+1.0	3
29	3.77	+1.0	3
40	1.00	+1.0	6

Molecules considered for the geometry optimization: ^a Propanol. ^b Propionic acid. ^c Propionaldehyde. ^d Butanone. ^e Ethylacetate. ^f Ethoxyethane.

the simultaneous reproduction of the experimental data for the four thermodynamic properties considered could not be found. In this case, a higher weight was given to ρ_{liq} , an intermediate weight to ΔH_{vap} and ΔG_{wat} and a lower weight to ΔG_{che} . The parametrization involved about 200 000 simulation runs for a total computing time of about 14 CPU years on a heterogeneous cluster mostly composed of quad-core AMD Opteron 8380 CPUs.

The final reoptimized nonbonded interaction parameters are provided in Tables 4 (charges) and 5 (Lennard-Jones), and compared with the corresponding values in the S3A5 and S3A6 force fields³⁴ as well as a variant, i.e., an ether set labeled S3A6_w.³⁷ The latter set involves modified Lennard-Jones interaction parameters for the oxygen atom type OE as well as a slightly different charge set for the ether function, and was refined specifically for ethers and polyethers against pure-liquid properties, hydration free energies, and conformational properties. The definition of the S3A6_{OXY} force field is completed by (i) the single-atom Lennard-Jones interaction parameters corresponding to the 50 unaltered atom types of the S3A6 force field, see Table VII in ref 34; (ii) the selection matrix for single-

atom parameter combinations defining non-hydrogen-bonding, uncharged hydrogen-bonding, and charged hydrogen-bonding pair Lennard-Jones parameters in the S3A6 force field, see Table VIII in ref 34; and (iii) the residue topology building blocks of the GROMOS force field,⁷ solely altered in the assignment of bond and bond-angle types (Figure 1 and Table 3) as well as atomic charges (Table 4) for the oxygen functions.

The details concerning the simulations required for the evaluation of ρ_{liq} , ΔH_{vap} , ΔG_{wat} , and ΔG_{che} are provided in the following sections. Error estimates on the calculated quantities were evaluated by block averaging.¹ For the pure-liquid properties, ρ_{liq} and ΔH_{vap} , the errors were always below 1% and are not reported. For the solvation properties, ΔG_{wat} and ΔG_{che} , the total error was estimated by weighted summation of error contributions evaluated separately for the simulations at the successive λ -values (see section II.5).

II.2. Simulation Protocol. All simulations were performed using the GROMOS MD++ program,⁶⁹ release version 0.3.0. The GROMOS force-field parameter sets considered are S3A5 and S3A6,³⁴ the variant S3A6_w for ethers,³⁷ and the new

Table 4. Partial Charges of the Atoms within the Different Oxygen Functions in the GROMOS Force Field^a

chemical function	IAC	atom type	partial atomic charges			
			S3A5 [<i>e</i>]	S3A6 [<i>e</i>]	S3A6 _{variant} [<i>e</i>]	S3A6 _{OXY} [<i>e</i>]
alcohol	21	H	0.403	0.408		0.410
	3	OA	−0.611	−0.674		−0.700
	13–18	CHn	0.208	0.266		0.290
ether	4	OE	−0.324	−0.324	0.420 ^b	−0.580
	13–18	CHn	0.162	0.162	0.210 ^b	0.290
aldehyde	12	C				0.375
	20	HC				0.100
	1	O				0.475
ketone	1	O	−0.450	−0.450		−0.540
	12	C	0.450	0.450		0.540
acid	12	C	0.658	0.330		0.550
	1	O	−0.450	−0.450		−0.550
	3	OA	−0.611	−0.288		−0.410
	21	H	0.403	0.408		0.410
ester	13–18	CHn	0.160	0.266 ^c		0.290
	4	OE	−0.360	−0.069 ^c		−0.370
	1	O	−0.380	−0.450 ^c		−0.550
	12	C	0.580	0.253 ^c		0.630

^a The integer atom code (IAC) and the corresponding atom type are also indicated.³⁴ Each set of charges defines a single charge group. The S3A5 and S3A6 force fields³⁴ as well as the variant S3A6_W for ethers³⁷ and the parameter set S3A6_{OXY} derived in this work are shown. Empty entries correspond to parameters not available in the given set. ^b Variant labeled S3A6_W, introduced by Winger et al.³⁷, for the simulation of polyethers, to be used with OE parameters of the same set (Table 5). ^c Introduced by Chandrasekhar et al.³³ for the simulation of esters and possibly lipids (entry q1 in the second Table of ref 33).

Table 5. Lennard-Jones Interaction Parameters for the Three Oxygen Types Used in the Simulation of the Chemical Functions Considered in This Work^a

force field	IAC	atom type	$C_6^{1/2}$ [(kJ mol ^{−1} nm ⁶) ^{1/2}]	$C_{12}^{1/2}$ [10 ^{−3} (kJ mol ^{−1} nm ¹²) ^{1/2}]		
				I	II	III
S3A5(6)	1	O	0.04756	1.000	1.130	
				
	3	OA	0.04756	1.100	1.227	
	4	OE	0.04756	1.100	1.227	
				
S3A6 _W	4	OE	0.06313	2.148	1.227	1.748
				
S3A6 _{OXY}	1	O	0.04136	0.995	1.100	
				
	3	OA	0.04500	1.150	1.350	
	4	OE	0.04123	1.529	1.529	

^a The integer atom type code (IAC) and corresponding atom type³⁴ are indicated along with the single-atom Lennard-Jones interaction parameters $C_6^{1/2}$ and $C_{12}^{1/2}$ entering the GROMOS geometric-mean combination rule.⁷ The parameters $C_{12,I}^{1/2}$, $C_{12,II}^{1/2}$, and $C_{12,III}^{1/2}$ refer to non-hydrogen-bonding, uncharged hydrogen-bonding, and charged hydrogen-bonding interactions. The indicated parameters correspond to the S3A5 and S3A6 force fields,³⁴ to a variant S3A6_W for ethers,³⁷ and to the parameter set S3A6_{OXY} derived in this work. Empty entries correspond to parameters not available in the given set.

parameter set S3A6_{OXY} developed in the present work. Note that in the case of ester compounds, the charge set corresponding to the S3A6 force field is the one developed by Chandrasekhar et al.

(entry q1 of the second table of ref 33). The solvent models considered are the SPC water model⁵⁸ and the GROMOS S3A6 cyclohexane model originally developed by Schuler et al.³¹

All simulations, including the gas-phase simulations, were carried out under periodic boundary conditions based on cubic computational boxes. Newton's equations of motion were integrated using the leapfrog scheme⁷⁰ with a time step of 2 fs. All bond lengths were constrained by application of the SHAKE procedure⁷¹ with a relative geometric tolerance of 10^{-4} . The temperature was maintained close to its reference value of 298.15 K (254 K for DME) by weak-coupling to external baths⁵ using a relaxation time of 0.1 ps. In all simulations, including the gas-phase simulations, distinct temperature baths were used for the translational and for the internal and rotational degrees of freedom of the molecules. Note that a joint coupling to a single temperature bath was used instead in ref 34 for both types of simulations, which explains the presence of small differences between the data reported therein and the present data for the 53A5 and 53A6 force fields (only significant for the gas-phase simulations). Except for the gas-phase simulations, which were performed at a constant volume, all simulations were carried out at constant pressure. The pressure was maintained close to its reference value of 1 bar by isotropic weak-coupling of the atomic coordinates and box dimensions to a pressure bath⁵ using a relaxation time of 0.5 ps. The isothermal compressibilities involved in the pressure coupling were set to 4.575×10^{-4} ($\text{kJ mol}^{-1} \text{nm}^{-3}$)⁻¹ for the simulations in water and to 11.2×10^{-4} ($\text{kJ mol}^{-1} \text{nm}^{-3}$)⁻¹ for the simulations in cyclohexane, or set equal to the experimental compressibility for the pure liquids (Table 2). The center of mass motion was removed every 100 ps. The nonbonded interactions were computed using a twin-range scheme,^{2,7} with short- and long-range cutoff distances set to 0.8 and 1.4 nm, respectively, and an update frequency of five time steps for the short-range pairlist and intermediate-range interactions. A reaction-field correction^{59,72} was applied to account for the mean effect of electrostatic interactions beyond the long-range cutoff distance, using relative dielectric permittivities of 61 for the simulations in water⁷³ and 6 for the simulations in cyclohexane, or set equal to the experimental permittivity value for the pure liquids (Table 2). The reaction-field self-term and excluded-atom-term contributions⁷⁴ to the energy, forces, and virial were included as described in ref 69.

II.3. Pure-Liquid Simulations. The initial coordinates for the simulations of the pure liquids were generated by randomly placing 512 molecules in cubic computational boxes of dimensions appropriate for the experimental density of the liquid. After energy minimization, the systems were equilibrated, first at constant volume (0.25 ns) and then at constant pressure (1 ns). The production runs at constant pressure used for the calculation of ρ_{liq} and ΔH_{vap} covered an additional 2 ns.

II.4. Gas-Phase Simulations. The estimation of the gas-phase intramolecular energies is required for the calculation of ΔH_{vap} . These gas-phase simulations were carried out as described in previous work,^{30,31,34} by simulating systems in which the individual molecules are initially placed very far apart from each other within a periodic box. The initial coordinates for these simulations were generated by randomly placing 512 molecules in cubic computational boxes of edge length ~ 750 nm, respecting a minimal intermolecular distance of 50 nm. This value is sufficient to ensure that the distances between atoms within different molecules do exceed the long-range cutoff distance of 1.4 nm throughout the simulations. This setup mimics a gas-phase situation while providing more statistics compared to a single-molecule simulation, and permitting a coupling to a nonstochastic thermostat. The systems were equilibrated at

constant volume for 0.1 ns, followed by 0.2 ns of production. The enthalpy of vaporization ΔH_{vap} was calculated as the difference between the average potential energy per molecule in the gas-phase and pure-liquid simulations, expressed on a per mole basis and increased by RT , where R is the ideal-gas constant and T is the absolute temperature. This corresponds to a standard-state definition involving a reference pressure of 1 bar for both the gas-phase and liquid standard states, as recommended by IUPAC.⁷⁵ The term $M_{\text{liq}}\rho_{\text{liq}}^{-1}$, where M_{liq} is the molar mass of the compound, accounting for the volume-pressure enthalpy contribution of the pure liquid, is in all cases very small and was neglected.

II.5. Solvation Free-Energy Calculations. Simulations in water and cyclohexane were carried out in order to evaluate the corresponding solvation free energies ΔG_{wat} and ΔG_{che} . The initial coordinates of these simulations were generated by randomly placing one solute molecule and 1000 or 300 molecules of water or cyclohexane, respectively, in cubic computational boxes of dimensions appropriate for the experimental density of the pure solvent. After energy minimization, the systems were equilibrated as described for the pure liquids (section II.3). For the free-energy calculations, the solute–solvent interactions were perturbed using a coupling-parameter λ based on a soft-core scheme,⁷⁶ where $\lambda = 0$ corresponds to full and $\lambda = 1$ to vanishing solute–solvent interactions. The electrostatic soft-core parameter was set to 0.5 nm and the Lennard-Jones soft-core parameter to 0.5. Thermodynamic integration⁷⁷ was applied on the basis of 21 equidistant λ values and trapezoidal integration in a semi-sequential way; i.e., coordinates obtained after 50 ps of equilibration at λ were used as initial coordinates for the simulation at $\lambda + \Delta\lambda$. For each λ value, the system was equilibrated for 0.1 ns, followed by a production simulation of 0.8 ns. The estimates of ΔG_{wat} and ΔG_{che} calculated in this way, expressed on a per mole basis, were compared directly to experimental data according to a standard-state definition involving identical reference molar volumes, e.g., $1 \text{ dm}^3 \text{ mol}^{-1}$, for the gas-phase and solute standard states. This procedure performed well for all compounds, with the exception of DXE. For this compound, an additional stochastic thermostat was required for appropriate sampling.

III. RESULTS AND DISCUSSION

The results of the calculations involving the different parameter sets considered (Tables 3–5) are reported and compared to experimental data in Tables 6–11, ordered by chemical function. The overall quality of the parametrization for the different classes of compounds is also characterized in Table 12 in the form of root-mean-square deviations (RMSD) and average deviations (AVED) of the values of the different observables relative to the experimental values. The comparison is also illustrated graphically in Figure 2. For each class of compounds, a comparison of the results obtained using the different force fields is made. In nearly all cases, the present reparametrization results in a significant improvement. The word significant is used here with reference to differences on the order of at least 1% in terms of the density or at least $k_{\text{B}}T$ (2.5 kJ mol^{-1} at room temperature) in terms of energetic quantities.

III.1. Alcohols. The parameters for the alcohol function were calibrated on the basis of the primary alcohols ETL and PPL, and their transferability was subsequently tested using the other primary alcohols MTL, BTL, PTL, HXL, HPL, and OTL, the secondary alcohols 2PPL, 2BTL, 2PTL, 3PTL, and CHXL, and

Table 6. Comparison between Experimental and Simulated Properties of the Alcohols^a

param. set	compound	ρ_{liq} (kg m ⁻³)	ΔH_{vap} (kJ mol ⁻¹)	ΔG_{wat} (kJ mol ⁻¹)	ΔG_{che} (kJ mol ⁻¹)
experiment	MTL	784 ^b	37.4 ^b	-21.4 ^c	-5.4 ^c
	ETL	785 ^b	42.3 ^b	-20.9 ^c	-10.8 ^c
	PPL	800 ^b	47.5 ^b	-20.6 ^c	-11.4 ^c
	BTL	806 ^b	52.3 ^b	-19.8 ^c	-14.7 ^c
	PTL	811 ^b	56.9 ^b	-18.7 ^c	-15.1 ^c
	HXL	815 ^b	61.9 ^b	-18.2 ^c	-22.2 ^c
	HPL	820 ^d	66.8 ^c	-17.7 ^c	-25.2 ^c
	OTL	822 ^b	71.0 ^b	-17.1 ^c	
	2PPL	780 ^b	45.5 ^b	-19.3 ^c	-9.9 ^c
	2BTL	802 ^b	49.6 ^b	-19.2 ^f	
	2PTL	805 ^b	53.1 ^b	-18.4 ^f	
	3PTL	816 ^b	53.1 ^b	-18.2 ^f	
	CHXL	968 ^b	62.0 ^b	-22.9 ^f	
	2M2P	781 ^b	46.8 ^b	-18.9 ^c	-12.3 ^c
	2M2B	805 ^b	50.2 ^b	-18.5 ^f	
53A5	MTL	811 [1.03]	41.7 {4.3}	-20.1 ± 1.0 {1.2}	-4.1 ± 0.7 {1.3}
	ETL	778 [0.99]	45.4 {3.1}	-15.5 ± 0.9 {5.4}	-8.2 ± 0.7 {2.7}
	PPL	787 [0.98]	49.8 {2.3}	-15.6 ± 1.2 {5.0}	-11.9 ± 0.9 {-0.5}
	BTL	796 [0.99]	54.7 {2.4}	-14.4 ± 1.7 {5.3}	-15.7 ± 1.1 {-1.0}
	PTL	803 [0.99]	59.9 {3.0}	-13.4 ± 1.5 {5.3}	-19.0 ± 1.0 {-3.9}
	HXL	808 [0.99]	65.2 {3.3}	-12.2 ± 1.4 {6.1}	-23.1 ± 1.1 {-0.9}
	HPL	811 [0.99]	70.1 {3.3}	-12.5 ± 1.4 {5.2}	-26.1 ± 1.2 {-0.9}
	OTL	815 [0.99]	75.2 {4.2}	-12.0 ± 1.7 {5.1}	-28.4 ± 1.1 {-}
	2PPL	738 [0.95]	44.3 {-1.2}	-10.6 ± 1.3 {8.7}	-9.2 ± 0.8 {0.7}
	2BTL	769 [0.96]	49.3 {-0.4}	-10.3 ± 1.4 {8.9}	-13.7 ± 0.9 {-}
	2PTL	779 [0.97]	54.2 {1.1}	-9.8 ± 1.2 {8.5}	-18.0 ± 0.9 {-}
	3PTL	784 [0.96]	53.9 {0.8}	-10.1 ± 1.4 {8.1}	-18.4 ± 1.2 {-}
	CHXL	903 [0.93]	60.4 {-1.6}	-13.2 ± 1.3 {9.7}	-23.2 ± 1.0 {-}
	2M2P	735 [0.94]	39.4 {-7.4}	-7.7 ± 1.5 {11.2}	-10.4 ± 0.9 {1.9}
	2M2B	772 [0.96]	45.4 {-4.8}	-7.3 ± 1.3 {11.2}	-14.6 ± 1.1 {-}
53A6	MTL	859 [1.10]	47.0 {9.6}	-22.2 ± 1.2 {-0.8}	-4.1 ± 0.7 {1.3}
	ETL	796 [1.01]	49.7 {7.4}	-19.3 ± 1.2 {1.6}	-8.1 ± 0.7 {2.7}
	PPL	797 [1.00]	53.9 {6.4}	-19.0 ± 1.5 {1.5}	-11.9 ± 0.9 {-0.5}
	BTL	804 [1.00]	58.9 {6.6}	-18.0 ± 1.3 {1.7}	-15.7 ± 1.1 {-0.9}
	PTL	808 [1.00]	64.0 {7.1}	-17.8 ± 1.5 {0.9}	-19.0 ± 1.0 {-3.9}
	HXL	811 [1.00]	68.9 {7.0}	-16.6 ± 1.7 {1.6}	-23.1 ± 1.1 {-0.9}
	HPL	815 [0.99]	73.1 {6.3}	-16.4 ± 1.6 {1.3}	-26.0 ± 1.2 {-0.9}
	OTL	817 [0.99]	78.0 {7.0}	-15.5 ± 1.5 {1.6}	-28.4 ± 1.1 {-}
	2PPL	745 [0.96]	48.2 {2.7}	-14.8 ± 1.3 {4.5}	-9.2 ± 0.8 {0.7}
	2BTL	773 [0.96]	52.8 {3.1}	-14.8 ± 1.4 {4.3}	-13.7 ± 0.9 {-}
	2PTL	786 [0.98]	58.4 {5.3}	-14.0 ± 1.2 {4.4}	-18.0 ± 0.9 {-}
	3PTL	789 [0.97]	57.8 {4.7}	-14.2 ± 1.5 {4.0}	-18.4 ± 1.2 {-}
	CHXL	909 [0.94]	64.2 {2.2}	-17.3 ± 1.5 {5.6}	-23.2 ± 1.0 {-}
	2M2P	742 [0.95]	43.6 {-3.2}	-12.5 ± 1.5 {6.4}	-10.4 ± 1.0 {1.9}
	2M2B	781 [0.97]	49.9 {-0.3}	-12.4 ± 1.1 {6.1}	-14.6 ± 1.1 {-}
53A6 _{OXY}	MTL	822.7 [1.05]	43.0 {5.6}	-21.7 ± 1.4 {-0.3}	-3.5 ± 0.7 {1.9}
	ETL	776.4 [0.99]	45.6 {3.3}	-19.5 ± 1.2 {1.5}	-6.2 ± 0.9 {4.7}
	PPL	781.0 [0.98]	49.5 {2.0}	-18.2 ± 1.7 {2.4}	-10.4 ± 1.1 {1.0}
	BTL	791.4 [0.98]	54.4 {2.1}	-16.5 ± 1.8 {3.3}	-14.4 ± 1.1 {0.3}
	PTL	796.4 [0.98]	59.7 {2.8}	-16.1 ± 1.8 {2.6}	-17.9 ± 1.3 {-2.8}
	HXL	803.0 [0.99]	64.6 {2.7}	-15.7 ± 1.8 {2.6}	-21.5 ± 1.5 {0.8}
	HPL	807.3 [0.98]	69.7 {2.9}	-14.3 ± 1.8 {3.4}	-23.5 ± 1.3 {1.7}
	OTL	810.6 [0.99]	74.6 {3.6}	-14.6 ± 2.1 {2.5}	-27.7 ± 1.3 {-}
	2PPL	733.5 [0.94]	44.2 {-1.3}	-13.9 ± 1.3 {5.4}	-7.7 ± 1.1 {2.2}
	2BTL	762.3 [0.95]	49.1 {-0.6}	-13.9 ± 1.4 {5.3}	-13.2 ± 1.2 {-}
	2PTL	774.1 [0.96]	54.0 {0.9}	-12.7 ± 1.4 {5.7}	-16.0 ± 1.1 {-}
	3PTL	779.1 [0.95]	53.5 {0.4}	-13.7 ± 1.5 {4.5}	-15.1 ± 1.4 {-}
	CHXL	900.6 [0.93]	60.6 {-1.4}	-16.0 ± 1.7 {6.9}	-22.9 ± 1.6 {-}
	2M2P	731.9 [0.94]	39.7 {-7.1}	-10.4 ± 1.4 {8.4}	-10.4 ± 1.1 {1.9}
	2M2B	768.6 [0.95]	45.3 {-4.9}	-10.7 ± 1.3 {7.8}	-14.5 ± 1.5 {-}

^a The properties are the pure-liquid density ρ_{liq} and enthalpy of vaporization ΔH_{vap} as well as the solvation free energies in water ΔG_{wat} and in cyclohexane ΔG_{che} at 1 bar and 298.15 K. The parameter sets considered are 53A5 and 53A6, as well as 53A6_{OXY} (present work). The ρ_{liq} ratio (simulation divided by experiment) is indicated between square brackets. The ΔH_{vap} , ΔG_{wat} and ΔG_{che} deviations (simulation minus experiment) are indicated between braces. Experimental values were taken from the following sources: ^b ref 65, ^c refs 90 and 91, ^d ref 92, ^e ref 89, ^f ref 93.

Table 7. Comparison between Experimental and Simulated Properties of the Ethers^a

param. set	compound	ρ_{liq} (kg m ⁻³)	ΔH_{vap} (kJ mol ⁻¹)	ΔG_{wat} (kJ mol ⁻¹)	ΔG_{che} (kJ mol ⁻¹)
experiment	DME ^b	722 ^c	21.5 ^d	-8.0 ^e	
	DEE	708 ^f	27.1 ^f	-7.4 ^e	-12.7 ^e
	MPH	736 ^d	27.6 ^g	-7.0 ^e	
	DXE	864 ^f	36.4 ^f	-20.2 ^e	
S3A5(6)	DME ^b	750 [1.04]	22.9 {1.4}	1.4 ± 1.0 {9.4}	-9.8 ± 0.8 {-}
	DEE	710 [1.00]	27.7 {0.6}	2.5 ± 1.1 {9.9}	-15.8 ± 1.0 {-3.1}
	MPH	726 [0.99]	29.1 {1.5}	2.1 ± 1.1 {9.1}	-15.4 ± 1.3 {-}
	DXE	855 [0.99]	37.4 {1.0}	-3.5 ± 1.6 {16.7}	-21.1 ± 1.2 {-}
S3A6 _W	DME ^b	749 [1.04]	25.4 {3.9}	-7.4 ± 1.0 {0.7}	-10.8 ± 0.8 {-}
	DEE	717 [1.01]	30.7 {3.6}	-2.7 ± 1.1 {4.7}	-16.7 ± 1.0 {-4.0}
	MPH	730 [0.99]	31.4 {3.7}	-1.5 ± 1.3 {5.4}	-18.2 ± 1.1 {-}
	DXE	852 [0.99]	41.7 {5.3}	-15.5 ± 1.8 {4.7}	-22.9 ± 1.5 {-}
S3A6 _{OXY}	DME ^b	713 [0.99]	24.0 {2.5}	-8.4 ± 1.1 {-0.4}	-7.3 ± 0.9 {-}
	DEE	691 [0.98]	28.0 {0.9}	-6.6 ± 1.6 {0.8}	-13.0 ± 1.4 {-0.3}
	MPH	704 [0.96]	29.3 {1.7}	-6.1 ± 1.5 {0.9}	-13.5 ± 1.2 {-}
	DXE	803 [0.93]	35.7 {-0.7}	-18.5 ± 1.8 {1.7}	-16.9 ± 1.5 {-}

^aThe properties are the pure-liquid density ρ_{liq} and enthalpy of vaporization ΔH_{vap} as well as the solvation free energies in water ΔG_{wat} and in cyclohexane ΔG_{che} at 1 bar and 298.15 K. The parameter sets considered are S3A5(6) and the variant S3A6_W, as well as S3A6_{OXY} (present work). The ρ_{liq} ratio (simulation divided by experiment) is indicated between square brackets. The ΔH_{vap} , ΔG_{wat} , and ΔG_{che} deviations (simulation minus experiment) are indicated between braces. ^bAt 254 K. Experimental values were taken from the following sources: ^cref 94, ^dref 92, ^eref 90 and 91, ^fref 65, ^gref 89.

the tertiary alcohols 2M2P and 2M2B. The calculated properties are compared to experimental data in Table 6.

Considering the primary alcohols beyond MTL, the three sets (S3A5, S3A6, and S3A6_{OXY}) reproduce well the experimental ρ_{liq} and ΔG_{che} . Although parameters appropriate for the longer-chain aliphatic alcohols do not appear to be transferable to MTL, no additional effort was invested in this compound considering the availability of a special parameter set for MTL within GROMOS.⁷⁸ For the secondary and tertiary alcohols, the agreement with experimental results in terms of ΔG_{che} (only two experimental values available) is also good. However, the liquid densities of these compounds are underestimated (by about 2–7%) for the three parameter sets.

Considering all alcohols, the calculated ΔH_{vap} and ΔG_{wat} differ significantly between the S3A5 and S3A6 parameter sets. On the one hand, the experimental ΔH_{vap} is reasonably well reproduced by S3A5 (RMSD of 3.4 kJ mol⁻¹), but this quantity is overestimated by S3A6 (RMSD of 5.8 kJ mol⁻¹). On the other hand, the experimental ΔG_{wat} is reasonably well reproduced by S3A6 (RMSD of 3.7 kJ mol⁻¹) but underestimated in magnitude by S3A5 (RMSD of 7.5 kJ mol⁻¹). These observations are not surprising considering that the S3A5 set was calibrated to reproduce primarily pure-liquid properties and the S3A6 set calibrated to reproduce primarily solvation properties. However, as evidenced by the results obtained using the S3A6_{OXY} parameter set, these two requirements are actually not entirely incompatible, provided that the C₆ parameter is also included in the optimization procedure. The latter set is as accurate as S3A5 in terms of ΔH_{vap} (RMSD 3.4→3.3 kJ mol⁻¹) and only slightly less accurate than S3A6 in terms of ΔG_{wat} (RMSD 3.7→4.8 kJ mol⁻¹).

Considering primary, secondary, and tertiary alcohols separately, the deviations from experimental results in terms of ΔH_{vap} and ΔG_{wat} are largely systematic within each of the three parameter sets. ΔH_{vap} is typically overestimated for primary and, to a lesser extent, secondary alcohols, while this quantity is systematically underestimated for tertiary alcohols.

III.2. Ethers. The parameters for the ether function in S3A6_{OXY} were calibrated on the basis of the topologically symmetric ethers DME and DEE, and their transferability subsequently tested using the asymmetric ether MPH and the diether DXE. Note that the parameter sets S3A5 and S3A6 are identical for these compounds and were only optimized against pure-liquid properties, because no ether group is found in amino acid side chains. In this case, the set will be referred to as S3A5(6). Note also that, in S3A6_{OXY}, the Lennard-Jones interaction parameters of the atom type OE (ether or ester oxygen) were calibrated exclusively considering esters (section III.6), and not ethers. The parameter refinement for the latter compounds thus exclusively involved the partial charges. The calculated properties are compared to experimental data in Table 7.

The S3A5(6) parameter set reproduces well the liquid properties ρ_{liq} and ΔH_{vap} , as well as ΔG_{che} for which only one experimental value is available, but it is quite inaccurate in terms of ΔG_{wat} . Here again, the S3A6_{OXY} parameter set is marginally less accurate than S3A5(6) in terms of ΔH_{vap} (RMSD 1.2→1.6 kJ mol⁻¹), while it achieves a significantly improved agreement with experimental values in terms of ΔG_{wat} (RMSD 11.7→1.1 kJ mol⁻¹). Work is currently in progress to further improve the description of diethers, in which a recalibration of the torsional potential associated with the O–C–C–O dihedral angle might be required to reproduce the experimental relative stability of different conformers.⁷⁹ Note finally that the S3A6_W variant³⁷ represented a significant improvement over S3A5(6) in terms of ΔG_{wat} . However, it is still slightly less accurate compared to S3A6_{OXY} in terms of this property, and shows a more significant deviation for ΔH_{vap} .

III.3. Aldehydes. The parameters for the aldehyde function in S3A6_{OXY} were calibrated on the basis of the compound EAL, and their transferability was subsequently tested using the compounds PAL and BAL. The hydrogen atom type HC, originally introduced for aromatic ring hydrogen atoms and characterized by nonzero Lennard-Jones interaction parameters, was selected

Table 8. Comparison between Experimental and Simulated Properties of the Aldehydes^a

param. set	compound	ρ_{liq} (kg m ⁻³)	ΔH_{vap} (kJ mol ⁻¹)	ΔG_{wat} (kJ mol ⁻¹)	ΔG_{che} (kJ mol ⁻¹)
experiment	EAL	778 ^b	26.1 ^b	-14.6 ^c	[-]
	PAL	791 ^b	29.6 ^b	-14.4 ^c	[-]
	BAL	796 ^b	33.6 ^b	-13.3 ^c	[-]
53A6 _{OXY}	EAL	789 [1.01]	30.5 { 4.4}	-13.3 ± 1.0 { 1.3}	-7.2 ± 0.7 {-}
	PAL	779 [0.99]	34.1 { 4.5}	-11.4 ± 1.2 { 3.0}	-10.6 ± 0.8 {-}
	BAL	790 [0.99]	38.5 { 4.8}	-11.3 ± 1.4 { 2.0}	-13.3 ± 1.1 {-}

^aThe properties are the pure-liquid density ρ_{liq} and enthalpy of vaporization ΔH_{vap} as well as the solvation free energies in water ΔG_{wat} and in cyclohexane ΔG_{che} at 1 bar and 298.15 K. The parameter set considered is 53A6_{OXY} (present work). The ρ_{liq} ratio (simulation divided by experiment) is indicated between square brackets. The ΔH_{vap} , ΔG_{wat} , and ΔG_{che} deviations (simulation minus experiment) are indicated between braces. Experimental values were taken from the following sources: ^b ref 65, ^c ref 93.

Table 9. Comparison between Experimental and Simulated Properties of the Ketones^a

param. set	compound	ρ_{liq} (kg m ⁻³)	ΔH_{vap} (kJ mol ⁻¹)	ΔG_{wat} (kJ mol ⁻¹)	ΔG_{che} (kJ mol ⁻¹)
experiment	PPN	784 ^b	31.3 ^b	-16.1 ^c	-11.2 ^c
	BTN	800 ^b	34.5 ^b	-15.7 ^c	-14.6 ^c
	2PN	802 ^b	38.4 ^b	-14.8 ^c	-17.5 ^c
	3PN	809 ^b	38.5 ^b	-14.3 ^c	-18.0 ^c
	2HN	807 ^b	42.9 ^b	-13.8 ^c	-20.0 ^c
	3HN	815 ^d	42.5 ^d		
53A5(6)	PPN	824 [1.05]	31.6 { 0.3}	-8.2 ± 0.9 { 7.9}	-13.6 ± 0.9 {-2.5}
	BTN	810 [1.01]	34.6 { 0.1}	-6.3 ± 1.0 { 9.4}	-16.3 ± 0.9 {-1.8}
	2PN	814 [1.01]	39.5 { 1.1}	-4.7 ± 1.3 { 10.1}	-20.8 ± 1.0 {-3.3}
	3PN	804 [0.99]	37.8 {-0.7}	-4.9 ± 1.1 { 9.4}	-19.4 ± 1.0 {-1.4}
	2HN	817 [1.01]	44.1 { 1.2}	-5.4 ± 1.4 { 8.3}	-24.7 ± 1.1 {-4.7}
	3HN	807 [0.99]	42.4 {-0.1}	-1.8 ± 1.5 {-}	-22.4 ± 1.0 {-}
53A6 _{OXY}	PPN	813 [1.04]	32.9 { 1.6}	-13.8 ± 1.2 { 2.3}	-10.8 ± 0.8 { 0.4}
	BTN	799 [1.00]	35.5 { 1.0}	-13.0 ± 1.5 { 2.7}	-13.9 ± 1.1 { 0.7}
	2PN	804 [1.00]	40.6 { 2.2}	-11.8 ± 1.6 { 3.0}	-18.7 ± 0.9 {-1.2}
	3PN	794 [0.98]	38.7 { 0.1}	-11.0 ± 1.4 { 3.3}	-17.8 ± 1.1 { 0.2}
	2HN	809 [1.00]	45.2 { 2.3}	-12.1 ± 1.4 { 1.7}	-23.4 ± 1.1 {-3.4}
	3HN	799 [0.98]	43.3 { 0.8}	-9.9 ± 1.5 {-}	-19.8 ± 1.3 {-}

^aThe properties are the pure-liquid density ρ_{liq} and enthalpy of vaporization ΔH_{vap} as well as the solvation free energies in water ΔG_{wat} and in cyclohexane ΔG_{che} at 1 bar and 298.15 K. The parameter sets considered are 53A5(6) as well as 53A6_{OXY} (present work). The ρ_{liq} ratio (simulation divided by experiment) is indicated between square brackets. The ΔH_{vap} , ΔG_{wat} , and ΔG_{che} deviations (simulation minus experiment) are indicated between braces. Experimental values were taken from the following sources: ^b ref 65, ^c ref 90 and 91, ^d ref 89.

to represent the hydrogen atom of this functional group. Note that the Lennard-Jones interaction parameters of the atom type O (carbonyl oxygen) were calibrated exclusively considering ketones (section III.4), and not aldehydes. The parameter refinement for the latter compounds thus exclusively involved the partial charges. The calculated properties are compared to experimental data in Table 8. The experimental ρ_{liq} and ΔG_{wat} are very well reproduced, while ΔH_{vap} is systematically overestimated by about 4.5 kJ mol⁻¹.

III.4. Ketones. The parameters for the ketone function in 53A6_{OXY} were calibrated on the basis of the compounds PPN and BTN, and their transferability was subsequently tested using the compounds 2PN, 3PN, 2HN, and 3HN. Note that the parameter sets 53A5 and 53A6 are identical for these compounds and were only optimized against pure-liquid properties, because no ketone group is found in the amino acid side chains. In this case, the set will be referred to as 53A5(6). The calculated properties are compared to experimental data in Table 9.

Here again, the 53A6_{OXY} parameter set reproduces the ρ_{liq} and ΔG_{che} very well, slightly better than 53A5(6), and is only marginally less accurate than 53A5(6) in terms of ΔH_{vap} (RMSD 0.7→1.5 kJ mol⁻¹), while it achieves a significantly improved agreement with experimental values in terms of ΔG_{wat} (RMSD 9.1→2.7 kJ mol⁻¹).

III.5. Carboxylic Acids. The parameters for the carboxylic acid function in 53A6_{OXY} were calibrated on the basis of the compound ACA, and their transferability was subsequently tested using the compounds PPA and BTA. Note that the Lennard-Jones interaction parameters of the atom types O (carbonyl oxygen) and OA (alcohol or carboxylic acid oxygen) were calibrated exclusively considering ketones and alcohols, respectively (sections III.4 and III.1), and not carboxylic acids. The parameter refinement for the latter compounds thus exclusively involved the partial charges. The calculated properties are compared to experimental data in Table 10.

Similarly to the situation encountered for alcohols (section III.1), the experimental ΔH_{vap} is reasonably well reproduced by

Table 10. Comparison between Experimental and Simulated Properties of the Carboxylic Acids^a

param. set	compound	ρ_{liq} (kg m ⁻³)	ΔH_{vap} (kJ mol ⁻¹)	ΔG_{wat} (kJ mol ⁻¹)	ΔG_{che} (kJ mol ⁻¹)
experiment	ACA	1044 ^b	51.6 ^c	-28.3 ^d	-7.2 ^d
	PPA	988 ^b	58.6 ^c	-27.1 ^d	-15.8 ^d
	BTA	953 ^b	57.3 ^c	-26.6 ^d	
53A5	ACA	1148 [1.10]	48.0 { -3.6 }	-17.2 ± 1.1 { 11.1 }	-14.2 ± 0.9 { -7.0 }
	PPA	1034 [1.05]	50.6 { -6.7 }	-16.0 ± 1.4 { 11.1 }	-17.4 ± 1.0 { -1.6 }
	BTA	992 [1.04]	55.3 { -2.7 }	-13.4 ± 1.5 { 13.2 }	-20.9 ± 1.1 { - }
53A6	ACA	1147 [1.10]	64.2 { 12.6 }	-28.9 ± 1.3 { -0.6 }	-14.9 ± 1.0 { -7.7 }
	PPA	1029 [1.04]	67.8 { 10.5 }	-28.4 ± 1.3 { -1.3 }	-17.6 ± 1.0 { -1.8 }
	BTA	990 [1.04]	72.7 { 14.7 }	-27.3 ± 1.8 { -0.7 }	-20.5 ± 0.9 { - }
53A6 _{OXY}	ACA	1077.7 [1.03]	57.8 { 6.2 }	-24.3 ± 1.4 { 4.0 }	-9.9 ± 1.3 { -2.7 }
	PPA	975.6 [0.99]	61.3 { 4.0 }	-22.7 ± 1.5 { 4.4 }	-14.9 ± 1.3 { 0.9 }
	BTA	950.0 [1.00]	66.5 { 8.5 }	-21.4 ± 1.8 { 5.2 }	-17.9 ± 1.2 { - }

^aThe properties are the pure-liquid density ρ_{liq} and enthalpy of vaporization ΔH_{vap} as well as the solvation free energies in water ΔG_{wat} and in cyclohexane ΔG_{che} at 1 bar and 298.15 K. The parameter sets considered are 53A5 and 53A6, as well as 53A6_{OXY} (present work). The ρ_{liq} ratio (simulation divided by experiment) is indicated between square brackets. The ΔH_{vap} , ΔG_{wat} and ΔG_{che} deviations (simulation minus experiment) are indicated between braces. Experimental values were taken from the following sources: ^b ref 65, ^c ref 95, ^d refs 90 and 91.

Table 11. Comparison between Experimental and Simulated Properties of the Esters^a

param. set	compound	ρ_{liq} (kg m ⁻³)	ΔH_{vap} (kJ mol ⁻¹)	ΔG_{wat} (kJ mol ⁻¹)	ΔG_{che} (kJ mol ⁻¹)
experiment	EAE	895 ^b	35.6 ^b	-13.1 ^c	-14.9 ^c
	MPE	915 ^d	35.6 ^c	-12.3 ^c	-15.5 ^c
	PAE	883 ^b	39.8 ^b	-12.0 ^c	-18.2 ^c
	BAE	876 ^b	43.6 ^b	-10.7 ^c	-20.7 ^c
53A5	EAE	923 [1.03]	38.0 { 2.4 }	0.8 ± 1.5 { 13.9 }	-22.4 ± 1.1 { -7.5 }
	MPE	926 [1.01]	37.3 { 1.7 }	1.0 ± 1.2 { 13.3 }	-22.1 ± 1.1 { -6.6 }
	PAE	907 [1.03]	42.7 { 2.9 }	2.6 ± 1.5 { 14.5 }	-23.9 ± 1.0 { -5.7 }
	BAE	896 [1.02]	47.9 { 4.3 }	3.5 ± 1.5 { 14.1 }	-29.3 ± 1.1 { -8.7 }
53A6	EAE	959 [1.07]	47.6 { 12.0 }	-16.4 ± 1.2 { -3.4 }	-21.3 ± 1.0 { -6.4 }
	MPE	965 [1.05]	48.8 { 13.2 }	-17.3 ± 1.2 { -5.1 }	-21.4 ± 0.9 { -5.8 }
	PAE	934 [1.06]	51.5 { 11.7 }	-15.7 ± 1.4 { -3.7 }	-25.1 ± 0.9 { -6.9 }
	BAE	918 [1.05]	56.0 { 12.4 }	-15.0 ± 1.5 { -4.3 }	-26.6 ± 1.2 { -6.0 }
53A6 _{OXY}	EAE	881.8 [0.99]	36.0 { 0.4 }	-9.6 ± 1.2 { 3.4 }	-17.4 ± 1.4 { -2.5 }
	MPE	883.1 [0.97]	36.0 { 0.4 }	-10.2 ± 1.4 { 2.1 }	-16.5 ± 1.3 { -1.0 }
	PAE	871.4 [0.99]	40.4 { 0.6 }	-10.3 ± 1.7 { 1.7 }	-19.9 ± 1.3 { -1.7 }
	BAE	866.1 [0.99]	45.3 { 1.7 }	-7.4 ± 1.9 { 3.2 }	-23.3 ± 1.5 { -2.7 }

^aThe properties are the pure-liquid density ρ_{liq} and enthalpy of vaporization ΔH_{vap} as well as the solvation free energies in water ΔG_{wat} and in cyclohexane ΔG_{che} at 1 bar and 298.15 K. The parameter sets considered are 53A5 and 53A6, as well as 53A6_{OXY} (present work). The ρ_{liq} ratio (simulation divided by experiment) is indicated between square brackets. The ΔH_{vap} , ΔG_{wat} and ΔG_{che} deviations (simulation minus experiment) are indicated between braces. Experimental values were taken from the following sources: ^b ref 65, ^c ref 90 and 91, ^d ref 92, ^e ref 89.

53A5 (RMSD of 5.2 kJ mol⁻¹), this quantity being overestimated by 53A6 (RMSD of 12.7 kJ mol⁻¹), while the experimental ΔG_{wat} is very well reproduced by 53A6 (RMSD of 0.9 kJ mol⁻¹), this quantity being underestimated in magnitude by 53A5 (RMSD of 11.8 kJ mol⁻¹). In contrast to the alcohols, however, neither of the two sets performs very well in terms of ρ_{liq} (overestimated by 4–10%) and ΔG_{che} (RMSD of 5.1–5.6 kJ mol⁻¹). The 53A6_{OXY} parameter set provides a compromise between the two sets, being somewhat less accurate than 53A5 in terms of ΔH_{vap} (RMSD 5.2→6.6 kJ mol⁻¹) and noticeably less accurate than 53A6 in terms of ΔG_{wat} (RMSD 0.9→4.6 kJ mol⁻¹). However, it represents a clear improvement over both sets in terms of ρ_{liq} (maximal deviation of 3%) and ΔG_{che} (RMSD 5.1–5.6→2.0 kJ mol⁻¹).

III.6. Esters. The parameters for the ester function in 53A6_{OXY} were calibrated on the basis of the compounds EAE and PAE, and

their transferability was subsequently tested using the compounds BAE and MPE. Note that the Lennard-Jones interaction parameters of the atom type O (carbonyl oxygen) were calibrated exclusively considering ketones (section III.4), and not esters. The parameter refinement for the latter compounds thus exclusively involved the atom type OE (ether or ester oxygen) and the partial charges. The calculated properties are compared to experimental data in Table 11.

In the context of esters, 53A5 does not perform very well. It systematically overestimates ρ_{liq} (by about 3%), ΔH_{vap} (RMSD of 3.0 kJ mol⁻¹), and the magnitude of ΔG_{che} (RMSD of 7.2 kJ mol⁻¹) and, most importantly, largely underestimates the magnitude of ΔG_{wat} (RMSD of 14.0 kJ mol⁻¹). The 53A6 set³³ provides a significant improvement in terms of solvation properties ΔG_{wat} and, to a lesser extent, ΔG_{che} , but at the cost of

Table 12. Root-Mean-Square Deviations (RMSD) of the Simulation Averaged Values of Different Observables (ρ_{liq} , ΔH_{vap} , ΔG_{wat} , and ΔG_{che}) Relative to Experimental Values^a

chemical function	parameter set	ρ_{liq}		ΔH_{vap}		ΔG_{wat}		ΔG_{che}	
		(kg m ⁻³)	(kg m ⁻³)	(kJ mol ⁻¹)	(kJ mol ⁻¹)	(kJ mol ⁻¹)	(kJ mol ⁻¹)	(kJ mol ⁻¹)	(kJ mol ⁻¹)
alcohols	S3A5	29.7	[−20.7]	3.4	[0.8]	7.5	[7.0]	1.8	[−0.1]
	S3A6	31.2	[−11.2]	5.8	[4.8]	3.7	[3.0]	1.9	[−0.1]
	S3A6 _{OXY}	33.8	[−24.1]	3.3	[0.7]	4.8	[4.1]	2.2	[1.3]
ethers	S3A5(6)	15.6	[2.8]	1.2	[1.1]	11.7	[11.3]	3.1	[3.1]
	S3A6 _W	15.7	[4.5]	4.2	[4.1]	4.3	[3.9]	4.0	[4.0]
	S3A6 _{OXY}	35.8	[−29.8]	1.6	[1.1]	1.1	[0.8]	0.3	[0.3]
aldehydes	S3A6 _{OXY}	10.0	[−2.3]	4.6	[4.6]	2.2	[2.1]		
ketones	S3A5(6)	18.4	[9.8]	0.7	[0.3]	9.1	[9.0]	3.0	[−2.7]
	S3A6 _{OXY}	14.9	[0.2]	1.5	[1.4]	2.7	[2.6]	1.7	[−0.7]
carboxylic acids	S3A5	69.4	[63.0]	5.2	[−4.5]	11.8	[11.8]	5.1	[−4.3]
	S3A6	66.8	[60.3]	12.7	[12.4]	0.9	[−0.9]	5.6	[−4.8]
	S3A6 _{OXY}	20.6	[5.7]	6.6	[6.0]	4.6	[4.5]	2.0	[−0.9]
esters	S3A5	21.7	[20.8]	3.0	[2.8]	14.0	[14.0]	7.2	[−7.1]
	S3A6	52.3	[51.8]	12.3	[12.3]	4.1	[−4.1]	6.3	[−6.3]
	S3A6 _{OXY}	19.1	[−17.0]	0.9	[0.8]	2.8	[2.6]	2.1	[−1.9]
all	S3A5	30.9	[15.1]	2.7	[0.2]	10.8	[10.6]	4.0	[−3.5]
	S3A6	36.9	[22.7]	6.6	[6.2]	5.9	[3.7]	4.0	[−3.4]
	S3A6 _{OXY} ^b	24.8	[−13.0]	2.8	[2.0]	3.2	[2.9]	1.7	[−0.4]
	S3A6 _{OXY} ^c	22.4	[−11.2]	3.1	[2.5]	3.0	[2.8]	1.7	[−0.4]

^aThe corresponding average deviations (AVED) are also indicated within brackets, corresponding to simulation minus experiment. ^bExcluding the aldehydes from the calculation. ^cIncluding the aldehydes in the calculation.

deteriorating the reproduction of the pure-liquid properties ρ_{liq} and ΔH_{vap} . The S3A6_{OXY} parameter set represents an improvement over S3A5 (as well as S3A6) in terms of all properties considered, namely, ρ_{liq} (underestimated by about 1 to a maximum of 3%), ΔH_{vap} (RMSD 3.0→0.9 kJ mol^{−1}), ΔG_{wat} (RMSD 14.0→2.8 kJ mol^{−1}), and ΔG_{che} (RMSD 7.2→2.1 kJ mol^{−1}). This improvement is expected to be particularly beneficial in the context of lipid simulations, where the S3A5 parameter set did not lead to entirely satisfactory results,^{33,38,53,80–82} which may also be related to the choice of Lennard-Jones interaction parameters between headgroup atoms.³⁸

III.7. Discussion. It has sometimes been suggested that a simultaneous reproduction, with a reasonable accuracy, of the pure-liquid properties of organic liquids (molecule in a low-polarity environment) and of their hydration free energies (molecule in a high-polarity environment) is incompatible with a mean-field representation of electronic polarization effects in classical force fields.^{83,84} According to the results presented here, this statement seems to lack general validity. Furthermore, if such an incompatibility is indeed observed for some classes of compounds, it may not originate solely from electronic polarization effects but could be related to the representation of hydrogen-bonding interactions.

The ability of the S3A6_{OXY} parameter set to reproduce both pure-liquid and hydration properties differs significantly among the functional groups considered. For example, for ketones, ethers, and esters, both types of properties are reproduced accurately. In particular, deviations on the order of 1–2 kJ mol^{−1} compared to experimental values for the hydration free

energies are within the statistical errors affecting these types of calculations and, for some compounds, within the errors associated with the experimental data itself. Therefore, for these compounds and considering the target properties ρ_{liq} , ΔH_{vap} , ΔG_{wat} , and ΔG_{che} , the present force field gives entirely satisfactory results, and an explicit representation of electronic polarizability does not appear to be required in this case. Of course, this explicit representation could still be beneficial for the description of other system properties such as dielectric or transport properties. Considering alcohols and carboxylic acids, however, although an improvement with respect to the previous versions of the force field was achieved, agreement with the experimental data is not as satisfactory. Interestingly, these compounds are also those presenting hydrogen-bond donor groups and are therefore capable of forming intermolecular hydrogen bonds in the pure-liquid state as well as of donating (rather than only accepting) hydrogen bonds to (from) water molecules in the hydrated state. Moreover, the argument usually invoked to justify the statement that implicitly polarizable classical models cannot reproduce pure-liquid and hydration properties simultaneously is that a model calibrated for a low-polarity environment will be “underpolarized” when placed in a higher-polarity environment, i.e., it will lack an additional effective dipole enhancement that should be caused by the polarization response to the new environment. Conversely, a model calibrated for a high-polarity environment will be “overpolarized” when placed in a lower polarity environment. This explanation appears reasonable but is incompatible with the observation that, for esters, the pure liquids of which have a relatively low dielectric permittivity (~5–6), the present

parametrization achieves agreement with experimental pure-liquid properties and hydration free-energies simultaneously, whereas for alcohol, the pure liquids of which have a relatively high dielectric permittivity (~ 25), it is apparently impossible to reach such an agreement. Finally, comparing the gas-phase static molecular polarizabilities of e.g. methylpropionate⁸⁵ ($\sim 8.53\text{--}8.79\text{ \AA}^3$) and propionic acid⁸⁵ ($\sim 6.80\text{--}6.96\text{ \AA}^3$), one would expect that polarizability effects are more important for an ester than for a carboxylic acid, although the present results, interpreted in terms of the above justification, would suggest the opposite conclusion. It seems therefore questionable to attribute the problem solely to the implicit treatment of electronic polarization effects. Classical force fields, irrespective of the way they account for molecular polarizability, involve many other approximations, ranging from the harmonic description of covalent interactions to the simplified and empirical treatment of both van der Waals interactions (e.g., *ad hoc* inverse-12th power form of the repulsion contribution to the Lennard-Jones interactions, neglect of dispersion effects beyond the inverse-sixth power term, *ad hoc* combination rules) and Coulombic interactions (e.g., distributed monopole approximation to the molecular charge density, cutoff and reaction-field correction). In particular, the apparent impossibility of reproducing simultaneously pure-liquid and hydration properties for alcohols and carboxylic acids rather hints toward deficiencies in the representation of hydrogen-bonding interactions as a mere resultant of Coulombic attraction and van der Waals repulsion. Of course, these differences may also have a component resulting from electronic polarizability. However, it should be kept in mind that even if the inclusion of explicit polarization turns out to remedy the problem, this is not sufficient to prove that electronic polarizability was its cause, considering that an increase in the flexibility of the force field functional form by introduction of new parameters will automatically improve agreement with experimental data after an appropriate parametrization.

IV. CONCLUSIONS

In the present work, a new parameter set (53A6_{OXY}) is developed for the GROMOS force field that combines reoptimized parameters for the oxygen functions (alcohols, ethers, aldehydes, ketones, carboxylic acids, and esters) with the current biomolecular force-field version³⁴ 53A6 for all other functions.

For the 35 oxygen compounds considered, the new 53A6_{OXY} parameter set provides a unified and satisfactory description of the two pure-liquid properties (ρ_{liq} , ΔH_{vap}) and the two solvation properties (ΔG_{wat} , ΔG_{che}) that were considered. Compared to 53A5 and 53A6, 53A6_{OXY} nearly systematically leads to comparable or improved agreement with experimental data in terms of these four quantities (the only noticeable exception being ΔG_{wat} for carboxylic acids).

The performance of the 53A6_{OXY} set relies on adding increased flexibility in the calibration task through (i) a simultaneous rather than separate refinement against experimental values of pure-liquid and solvation properties, (ii) a simultaneous rather than successive refinement of the Lennard-Jones interaction parameters and charges, and (iii) the allowance of moderate adjustments in the dispersive coefficients ($C_6^{1/2}$) of the Lennard-Jones interactions. Note that the latter adjustments are truly limited, with a change of the value $0.04756\text{ (kJ mol}^{-1}\text{ nm}^6)^{1/2}$ for all oxygen atoms in 53A5 and 53A6 to 0.04136 , 0.04500 , and $0.04123\text{ (kJ mol}^{-1}\text{ nm}^6)^{1/2}$ for the atom types O, OA, and OE, respectively, in 53A6_{OXY}.

Work is currently in progress following the same strategy to define improved interaction parameters for nitrogen-containing (amine and amide functions), sulfur-containing (thiol and sulfide functions), and aromatic compounds in the GROMOS force field. This extension would lead to an improved force field covering the entire range of amino acid side chains in natural polypeptides. A combination of 53A6_{OXY} with the recently reoptimized 53A6_{CARBO} parameter set for carbohydrates⁸⁶ is also planned. As with earlier versions of the GROMOS force field, the appropriateness of the new parametrizations remains to be validated in the context of biomolecular simulations.

AUTHOR INFORMATION

Corresponding Author

*Phone: +41 44 632 5503. Fax: + 41 44 632 1039. E-mail: bruno@igc.phys.chem.ethz.ch (B.A.C.H.); phil@igc.phys.chem.ethz.ch (P.H.H.).

ACKNOWLEDGMENT

The authors would like to thank Chris Oostenbrink, Alex de Vries, Alan Mark, and Alpesh Malde for valuable discussions. Many thanks are due to the "Brutus Team", and in particular Dr. Olivier Byrde, for steady support with the computer cluster. Financial support from the Swiss National Science Foundation (Grants 21-121895 and 200020-121913), from the National Center of Competence in Research (NCCR) in Structural Biology, and from the European Research Council (Grant 228076) are also gratefully acknowledged.

REFERENCES

- (1) Allen, M. P.; Tildesley, D. J. *Computer simulation of liquids*; Oxford University Press: New York, 1987.
- (2) van Gunsteren, W. F.; Berendsen, H. J. C. *Angew. Chem., Int. Ed.* **1990**, *29*, 992–1023.
- (3) van Gunsteren, W. F.; Bakowies, D.; Baron, R.; Chandrasekhar, I.; Christen, M.; Daura, X.; Gee, P.; Geerke, D. P.; Glättli, A.; Hünenberger, P. H.; Kastenholz, M. A.; Oostenbrink, C.; Schenk, M.; Trzesniak, D.; van der Vegt, N. F. A.; Yu, H. B. *Angew. Chem., Int. Ed.* **2006**, *45*, 4064–4092.
- (4) Berendsen, H. J. C. *Simulating the physical world.*; Cambridge University Press: Cambridge, U.K., 2007.
- (5) Berendsen, H. J. C.; Postma, J. P. M.; van Gunsteren, W. F.; di Nola, A.; Haak, J. R. *J. Chem. Phys.* **1984**, *81*, 3684–3690.
- (6) van Gunsteren, W. F.; Berendsen, H. J. C. *Mol. Phys.* **1977**, *34*, 1311–1327.
- (7) van Gunsteren, W. F.; Billeter, S. R.; Eising, A. A.; Hünenberger, P. H.; Krüger, P.; Mark, A. E.; Scott, W. R. P.; Tironi, I. G. *Biomolecular simulation: The GROMOS96 manual and user guide*; Verlag der Fachvereine: Zürich, Switzerland, 1996.
- (8) Scott, W. R. P.; Hünenberger, P. H.; Tironi, I. G.; Mark, A. E.; Billeter, S. R.; Fennen, J.; Torda, A. E.; Huber, T.; Krüger, P.; van Gunsteren, W. F. *J. Phys. Chem. A* **1999**, *103*, 3596–3607.
- (9) Engelsen, S. B.; Fabricius, J.; Rasmussen, K. *Acta Chem. Scand.* **1994**, *48*, 548–552.
- (10) Engelsen, S. B.; Fabricius, J.; Rasmussen, K. *Acta Chem. Scand.* **1994**, *48*, 553–565.
- (11) Gaedt, K.; Holtje, H. D. *J. Comput. Chem.* **1998**, *19*, 935–946.
- (12) Allinger, N. L. *J. Am. Chem. Soc.* **1989**, *111*, 8551–8566.
- (13) Allinger, N. L. *J. Am. Chem. Soc.* **1989**, *111*, 8566–8575.
- (14) Allinger, N. L. *J. Am. Chem. Soc.* **1989**, *111*, 8576–8582.
- (15) Allinger, N. L.; Chen, K.-H.; Lii, J.-H. *J. Comput. Chem.* **2003**, *24*, 1447–1472.

- (16) MacKerell, A. D.; Wiorkiewicz-kuczera, J.; Karplus, M. *J. Am. Chem. Soc.* **1995**, *117*, 11946–11975.
- (17) Mackerell, A. D., Jr.; Bashford, D.; Bellott, M.; Dunbrack, R. L.; Evanseck, J. D.; Field, M. J.; Fischer, S.; Gao, J.; Guo, H.; Ha, S.; Joseph-McCarthy, D.; Kuchnir, L.; Kuczera, K.; Lau, F. T. K.; Mattos, C.; Michnick, S.; Ngo, T.; Nguyen, D. T.; Prodhom, B.; Reiher, W. E.; Roux, B.; Schlenkrich, M.; Smith, J. C.; Stote, R.; Straub, J.; Watanabe, M.; Wiorkiewicz-Kuczera, J.; Yin, D.; Karplus, M. *J. Phys. Chem.* **1998**, *B*, 102.
- (18) Feller, S. E.; MacKerell, A. D. *J. Phys. Chem. B* **2000**, *104*, 7510–7515.
- (19) Hatcher, E. R.; Guvench, O.; MacKerell, A. D., Jr. *J. Phys. Chem. B* **2009**, *113*, 12466–12476.
- (20) Weiner, P. K.; Kollman, P. A. *J. Comput. Chem.* **1981**, *2*, 287–303.
- (21) Pearlman, D. A.; Case, D. A.; Caldwell, J. D.; Ross, W. S.; Cheatham, T. E., III; DeBolt, S.; Fergusson, D.; Seibel, G.; Kollman, P. *Comput. Phys. Commun.* **1995**, *91*, 1–41.
- (22) Cornell, W. D.; Cieplak, P.; Bayly, C. I.; Gould, I. R.; Merz, K. M.; Fergusson, D. M.; Spellmeyer, D. C.; Fox, T.; Caldwell, J. W.; Kollman, P. A. *J. Am. Chem. Soc.* **1995**, *117*, 5179–5197.
- (23) Kirschner, K. N.; Yongye, A. B.; Tschampel, S. M.; Gonzalez-Outterino, J.; Daniels, C. R.; Foley, B. L.; Woods, R. J. *J. Comput. Chem.* **2008**, *29*, 622–655.
- (24) Pranata, J.; Wierschke, S. G.; Jorgensen, W. L. *J. Am. Chem. Soc.* **1991**, *113*, 2810–2819.
- (25) Jorgensen, W. L.; Maxwell, D. S.; Tirado-Rives, J. *J. Am. Chem. Soc.* **1996**, *118*, 11225–11236.
- (26) Damm, W.; Frontera, A.; Tirado-Rives, J.; Jorgensen, W. *J. Comput. Chem.* **1997**, *18*, 1955–1970.
- (27) Kaminski, G. A.; Friesner, R. A.; Tirado-Rives, J.; Jorgensen, W. L. *J. Phys. Chem.* **2001**, *B*, 105.
- (28) Daura, X.; Mark, A. E.; van Gunsteren, W. F. *J. Comput. Chem.* **1998**, *19*, 535–547.
- (29) van Gunsteren, W. F.; Daura, X.; Mark, A. E. GROMOS force field. In *Encyclopedia of computational chemistry*; Schleyer, P., Ed.; John Wiley & Sons: Chichester, U.K., 1998; Vol. 2, pp 1211–1216.
- (30) Schuler, L. D.; van Gunsteren, W. F. *Mol. Simul.* **2000**, *25*, 301–319.
- (31) Schuler, L. D.; Daura, X.; van Gunsteren, W. F. *J. Comput. Chem.* **2001**, *22*, 1205–1218.
- (32) Chandrasekhar, I.; Kastenholz, M. A.; Lins, R. D.; Oostenbrink, C.; Schüller, L. D.; Tieleman, D. P.; van Gunsteren, W. F. *Eur. Biophys. J.* **2003**, *32*, 67–77.
- (33) Chandrasekhar, I.; Oostenbrink, C.; van Gunsteren, W. F. *Soft Mater.* **2004**, *2*, 27–45.
- (34) Oostenbrink, C.; Villa, A.; Mark, A. E.; van Gunsteren, W. F. *J. Comput. Chem.* **2004**, *25*, 1656–1676.
- (35) Soares, T. A.; Hünenberger, P. H.; Kastenholz, M. A.; Kräutler, V.; Lenz, T.; Lins, R. D.; Oostenbrink, C.; van Gunsteren, W. F. *J. Comput. Chem.* **2005**, *26*, 725–737.
- (36) Lins, R. D.; Hünenberger, P. H. *J. Comput. Chem.* **2005**, *26*, 1400–1412.
- (37) Winger, M.; de Vries, A. H.; van Gunsteren, W. F. *Mol. Phys.* **2009**, *107*, 1313–1321.
- (38) Poger, D.; van Gunsteren, W. F.; Mark, A. E. *J. Comput. Chem.* **2009**, *31*, 1117–1125.
- (39) Gee, P. J.; van Gunsteren, W. F. *Mol. Phys.* **2006**, *104*, 477–483.
- (40) Geerke, D. P.; van Gunsteren, W. F. *Mol. Phys.* **2007**, *105*, 1861–1881.
- (41) Walser, R.; Hünenberger, P. H.; van Gunsteren, W. F. *Proteins: Struct. Funct. Genet.* **2001**, *44*, 509–519.
- (42) Walser, R.; Hünenberger, P. H.; van Gunsteren, W. F. *Proteins: Struct. Funct. Genet.* **2002**, *48*, 327–340.
- (43) Smith, L. J.; Berendsen, H. J. C.; van Gunsteren, W. F. *J. Phys. Chem. B* **2004**, *108*, 1065–1071.
- (44) Geerke, D. P.; van Gunsteren, W. F. *ChemPhysChem* **2006**, *7*, 671–678.
- (45) Zagrovic, B.; Gattin, Z.; Kai-Chi Lau, J.; Huber, M.; van Gunsteren, W. F. *Eur. Biophys. J.* **2008**, *37*, 903–912.
- (46) Meier, K.; van Gunsteren, W. F. *J. Phys. Chem. A* **2010**, *114*, 1852–1859.
- (47) Allison, J. R.; van Gunsteren, W. F. *ChemPhysChem* **2009**, *10*, 3213–3228.
- (48) Eichenberger, A. P.; Gattin, Z.; Yalak, G.; van Gunsteren, W. F. *Helv. Chim. Acta* **2010**, *93*, 1857–1869.
- (49) Dolenc, J.; Oostenbrink, C.; Koller, J.; van Gunsteren, W. F. *Nucleic Acids Res.* **2005**, *33*, 725–733.
- (50) Perić-Hassler, L.; Hansen, H. S.; Baron, R.; Hünenberger, P. H. *Carbohydr. Res.* **2010**, *345*, 1781–1801.
- (51) Hansen, H. S.; Hünenberger, P. H. *J. Comput. Chem.* **2010**, *31*, 1–23.
- (52) Siwko, M. E.; de Vries, A. H.; Mark, A. E.; Kozubek, A.; Marrink, S. J. *Biophys. J.* **2009**, *96*, 3140–3153.
- (53) Horta, B. A. C.; Perić-Hassler, L.; Hünenberger, P. H. *J. Mol. Graphics Modell.* **2010**, *29*, 331–346.
- (54) Geerke, D. P.; van Gunsteren, W. F. *J. Chem. Theory Comput.* **2007**, *3*, 2128–2137.
- (55) Geerke, D. P.; van Gunsteren, W. F. *J. Phys. Chem. B* **2007**, *111*, 6425–6436.
- (56) Kunz, A.-P. E.; van Gunsteren, W. F. *J. Phys. Chem. A* **2009**, *113*, 11570–11579.
- (57) Lin, Z.; Kunz, A.-P.; van Gunsteren, W. F. *Mol. Phys.* **2010**, *108*, 1749–1757.
- (58) Berendsen, H. J. C.; Postma, J. P. M.; van Gunsteren, W. F.; Hermans, J. Interaction models for water in relation to protein hydration. In *Intermolecular Forces*; Pullman, B., Ed.; Reidel: Dordrecht, The Netherlands, 1981; pp 331–342.
- (59) Tironi, I. G.; Sperb, R.; Smith, P. E.; van Gunsteren, W. F. *J. Chem. Phys.* **1995**, *102*, 5451–5459.
- (60) Hermans, J.; Berendsen, H. J. C.; van Gunsteren, W. F.; Postma, J. P. M. *Biopolymers* **1984**, *23*, 1513–1518.
- (61) Daura, X.; Oliva, B.; Querol, E.; Aviles, F. X. *Proteins: Struct. Funct. Genet.* **1996**, *25*, 89–103.
- (62) Soares, T. A.; Daura, X.; Oostenbrink, C.; Smith, L. J.; van Gunsteren, W. F. *J. Biomol. NMR* **2004**, *30*, 407–422.
- (63) Oostenbrink, C.; Soares, T. A.; van der Vegt, N. F. A.; van Gunsteren, W. F. *Eur. Biophys. J.* **2005**, *34*, 273–284.
- (64) Slater, J. C.; Kirkwood, J. G. *Phys. Rev.* **1931**, *37*, 682–697.
- (65) Riddick, J. A.; Bunger, W. B.; Sakano, T. K. *Organic solvents, physical properties and methods of purification*; John Wiley & Sons: New York, 1986.
- (66) Frisch, M. J.; Trucks, G. W.; Schlegel, H. B.; Scuseria, G. E.; Robb, M. A.; Cheeseman, J. R.; Montgomery, J. A., Jr.; Vreven, T.; Kudin, K. N.; Burant, J. C.; Millam, J. M.; Iyengar, S. S.; Tomasi, J.; Barone, V.; Mennucci, B.; Cossi, M.; Scalmani, G.; Rega, N.; Petersson, G. A.; Nakatsuji, H.; Hada, M.; Ehara, M.; Toyota, K.; Fukuda, R.; Hasegawa, J.; Ishida, M.; Nakajima, T.; Honda, Y.; Kitao, O.; Nakai, H.; Klene, M.; Li, X.; Knox, J. E.; Hratchian, H. P.; Cross, J. B.; Bakken, V.; Adamo, C.; Jaramillo, J.; Gomperts, R.; Stratmann, R. E.; Yazyev, O.; Austin, A. J.; Cammi, R.; Pomelli, C.; Ochterski, J. W.; Ayala, P. Y.; Morokuma, K.; Voth, G. A.; Salvador, P.; D'Annunzio, J. J.; Zakrzewski, V. G.; Dapprich, S.; Daniels, A. D.; Strain, M. C.; Farkas, O.; Malick, D. K.; Rabuck, A. D.; Raghavachari, K.; Foresman, J. B.; Ortiz, J. V.; Cui, Q.; Baboul, A. G.; Clifford, S.; Cioslowski, J.; Stefanov, B. B.; Liu, G.; Liashenko, A.; Piskorz, P.; Komaromi, I.; Martin, R. L.; Fox, D. J.; Keith, T.; Al-laham, M. A.; Peng, C. Y.; Nanayakkara, A.; Challacombe, M.; Gill, P. M. W.; Johnson, B.; Chen, W.; Wong, M. W.; Gonzalez, C.; Pople, J. A. *Gaussian 03*, Revision D.01; Gaussian, Inc.: Wallingford, CT, 2004.
- (67) Villa, A.; Mark, A. E. *J. Comput. Chem.* **2002**, *23*, 548–553.
- (68) Horta, B. A. C.; de Vries, A. H.; Hünenberger, P. H. *J. Chem. Theory Comput.* **2010**, *6*, 2488–2500.
- (69) Christen, M.; Hünenberger, P. H.; Bakowies, D.; Baron, R.; Bürgi, R.; Geerke, D. P.; Heinz, T. N.; Kastenholz, M. A.; Kräutler, V.; Oostenbrink, C.; Peter, C.; Trzesniak, D.; van Gunsteren, W. F. *J. Comput. Chem.* **2005**, *26*, 1719–1751.
- (70) Hockney, R. W. *Methods Comput. Phys.* **1970**, *9*, 136–211.
- (71) Ryckaert, J.-P.; Ciccotti, G.; Berendsen, H. J. C. *J. Comput. Phys.* **1977**, *23*, 327–341.

- (72) Barker, J. A.; Watts, R. O. *Mol. Phys.* **1973**, *26*, 789–792.
- (73) Heinz, T. N.; van Gunsteren, W. F.; Hünenberger, P. H. *J. Chem. Phys.* **2001**, *115*, 1125–1136.
- (74) Heinz, T. N.; Hünenberger, P. H. *J. Chem. Phys.* **2005**, *123*, 034107/1–034107/19.
- (75) IUPAC *Quantities, Units and Symbols in Physical Chemistry, Green Book*, 2nd ed.; Blackwell Scientific Publications: Oxford, U. K., 1993.
- (76) Beutler, T. C.; Mark, A. E.; van Schaik, R.; Gerber, P. R.; van Gunsteren, W. F. *Chem. Phys. Lett.* **1994**, *222*, 529–539.
- (77) Kirkwood, J. G. *J. Chem. Phys.* **1935**, *3*, 300–313.
- (78) Walser, R.; Mark, A. E.; van Gunsteren, W. F.; Lauterbach, M.; Wipff, G. *J. Chem. Phys.* **2000**, *112*, 10450–10459.
- (79) Fuchs, P. F. J.; Horta, B. A. C.; Hünenberger, P. H. 2010, in preparation.
- (80) Pereira, C. S.; Lins, R. D.; Chandrasekhar, I.; Freitas, L. C. G.; Hünenberger, P. H. *Biophys. J.* **2004**, *86*, 2273–2285.
- (81) Chandrasekhar, I.; Bakowies, D.; Glättli, A.; Hünenberger, P. H.; Pereira, C.; van Gunsteren, W. F. *Mol. Simul.* **2005**, *31*, 543–548.
- (82) Pereira, C. S.; Hünenberger, P. H. *J. Phys. Chem. B* **2006**, *110*, 15572–15581.
- (83) Baker, C. M.; Lopes, P. E. M.; Zhu, X.; Roux, B.; McKerell, A. D. *J. Chem. Theory Comput.* **2010**, *6*, 1181–1198.
- (84) Zhong, Y.; Patel, S. *J. Phys. Chem. B* **2010**, *114*, 11076–11092.
- (85) Miller, K. J. *J. Am. Chem. Soc.* **1990**, *112*, 8533–8542.
- (86) Hansen, H. S.; Hünenberger, P. H. *J. Comput. Chem.* **2010**, submitted.
- (87) Börjesson, U.; Hünenberger, P. H. *J. Phys. Chem. B* **2004**, *108*, 13551–13559.
- (88) Wohlfahrt, C. Pure liquids: Data. In *Landolt-Börnstein. Numerical data and functional relationships in science and technology*; Madelung, O., Ed.; Springer: Berlin, Germany, 1991; Vol. 6, pp 5–228.
- (89) Majer, V.; Svoboda, V. *Enthalpies of vaporization of organic compounds: A critical review and data compilation*; Blackwell Scientific Publications: Oxford, U.K., 1985.
- (90) Hawkins, G. D.; Cramer, C. J.; Truhlar, D. G. *J. Phys. Chem. B* **1998**, *102*, 3257–3271.
- (91) Li, J.; Zhu, T.; Hawkins, G. D.; Winget, P.; Liotard, D. A.; Cramer, C. J.; Truhlar, D. G. *Theor. Chem. Acc.* **1999**, *103*, 9–63.
- (92) Lide, D. R. *CRC Handbook of Chemistry and Physics*, 80th ed.; CRC Press: Boca Raton, FL, 1999.
- (93) Gallicchio, E.; Zhang, L. Y.; Levy, R. M. *J. Comput. Chem.* **2001**, *23*, 517–529.
- (94) Wu, J.; Liu, Z.; Bi, S.; Meng, X. *J. Chem. Eng. Data* **2003**, *48*, 426–429.
- (95) Pedley, J. B.; Naylor, R. D.; Kirby, S. P. *Thermodynamical Data of Organic Compounds*; Chapman and Hall: London, U.K., 1986.